



BI-ORTHOGONALITY CONDITIONS FOR POWER FLOW ANALYSIS IN FLUID-LOADED ELASTIC CYLINDRICAL SHELLS: THEORY AND APPLICATIONS

L. S. Ledet^{1*}, S. V. Sorokin¹, J. B. Larsen², M. M. Lauridsen²

¹ Department of Mechanical and Manufacturing Engineering
Aalborg University, Fibigerstraede 16, Aalborg, DK-9220
Email: lledet10@student.aau.dk
Email: svs@m-tech.aau.dk

² Grundfos Holding A/S
Poul Due Jensens Vej 7, Bjerringbro, DK-8850
Email: janballelarsen@grundfos.com
Email: mmlauridsen@grundfos.com

ABSTRACT

The paper addresses the classical problem of time-harmonic forced vibrations of a fluid-loaded cylindrical shell considered as a multi-modal waveguide carrying infinitely many waves. Firstly, a modal method for formulation of Green's matrix is derived by means of modal decomposition. The method builds on the recent advances on bi-orthogonality conditions for multi-modal waveguides, which are derived here for an elastic fluid-filled cylindrical shell. Subsequently, modal decomposition is applied to the bi-orthogonality conditions to formulate explicit algebraic equations to express the modal amplitudes independently of each other. Secondly, the method is verified against results available in the literature and the convergence is studied as well. Thirdly, the work conducted in the same references is extended by employing this method to assess the near field energy distribution when the coupled vibro-acoustic waveguide is subjected to separate pressure and velocity excitations. Further, it has been found and justified that the bi-orthogonality conditions can be used as a 'root finder' to solve the dispersion equation. Finally, it is discussed how to predict the response of a fluid-filled shell when the excitation is imported from CFD-modelling of an operating pump.

1 INTRODUCTION

This paper is concerned with analysis of fluid- and structure borne noise in piping systems conveying a heavy acoustic medium, such as water or sewage. The field of acoustical and mechanical

noise in piping systems share many common interests e.g. by industrial partners as well as a wide range of Research Departments around the world. However, the main issue from the view point of the co-authors in this paper (Grundfos Holding A/S) is the sound emission and mechanical vibrations as these are directly related to comfort and fatigue durability. Consequently, it is essential to have an understanding of the acoustical and mechanical vibrations and how to suppress these to accommodate with vibrational demands. This immediately entails a coupled vibro-acoustic model to cope with the fluid-structure interaction.

For the coupled vibro-acoustic waveguide we employ the classical models of an infinite thin elastic cylindrical shell and an inviscid compressible fluid with no mean flow. In addition to this the model is restricted to time-harmonic forced vibrations. This is a classical problem considered in numerous publications with [1] and [2] being the most cited references on the subject. In these references the acoustic and mechanical vibrations are assessed by means of the energy flow, from which the dominant path(s) of energy transmission can be identified.

To analyse arbitrary forcing problems we employ Green's matrix method which is a well-known and widely acknowledged method used to recover the response of a given waveguide. This method does indeed have a wide range of applications and in relation to the scope of this paper it has been used in [3] to predict the near field energy distribution when applied to fundamental mechanical loading conditions. Similarly, it has been used in [4] to calculate the power flow when applied to acoustical loadings with the scope of mapping available CFD-data onto the shell.

However, the conventional method for formulating Green's matrix has certain convergence and accuracy limitations in predicting the near field energy distribution of such coupled vibro-acoustic waveguides. Thus the motivation of this paper is to develop a sustainable method for accurately and efficiently formulating Green's matrix.

The method developed throughout this paper is based on the recent advances on bi-orthogonality conditions for elastic multi-modal waveguides. These conditions have been facilitated in [5] to calculate the modal amplitudes of a straight elastic layer and similar in [6] to solve the classical Rayleigh-Lamb problem by means of modal decomposition. The latter reference is based on the work conducted by Achenbach in [7], from which the work of [8] also arises. Here the concept has been adapted to simple elastic multi-modal waveguides again with the scope of calculating the modal amplitudes by means of modal decomposition. In the present paper the work from the latter reference is extended to the more complex elastic multi-modal waveguide of a cylindrical shell conveying heavy fluid. The bi-orthogonality conditions for this waveguide are derived here and facilitated to decompose the equation system into a set of explicit algebraic equations for calculating modal amplitudes for, in general, five fundamental loading conditions.

The paper is structured as follows: Section 2 presents the governing equations, the orthogonality condition and the power flow equations for the fluid-filled shell. In section 3 the modal decomposition method is derived, starting with the derivation of the bi-orthogonality conditions and subsequently the formulation of Green's matrix for the fundamental loading conditions. Section 4 is devoted to justify of the modal decomposition method through a verification with respect to the work done in [3] and likewise study the convergence of the power flow for acoustical loadings. Section 5 contains an extension to the work in [3] by analysing the near field energy distribution with a converged pressure and velocity excitation applied at different locations along the radii. This section also contains a brief discussion of other useful properties of the bi-orthogonality conditions. Finally, section 6 briefly outlines the procedure for mapping CFD-data onto the vibro-acoustic model.

2 GOVERNING EQUATIONS

To assess vibrations of a fluid-filled shell we employ the standard formulation for the fluid-structure interaction problem for a thin elastic cylindrical shell loaded by an inviscid compressible fluid. The detailed derivations of the equations of motion from the action integral can be found in e.g. [3].

The free vibrations of a fluid-loaded shell are described through the following system of equations in the framework of Novozhilov-Gol'denveiser's shell theory.

$$\begin{aligned} -\frac{\partial^2 u_m}{\partial x^2} + \frac{1-\nu}{2} \frac{m^2}{R^2} u_m - \frac{1+\nu}{2} \frac{m}{R} \frac{\partial v_m}{\partial x} - \frac{\nu}{R} \frac{\partial w_m}{\partial x} + \frac{\rho_{str}(1-\nu^2)}{E} \frac{\partial^2 u_m}{\partial t^2} = 0 \\ \frac{1+\nu}{2} \frac{m}{R} \frac{\partial u_m}{\partial x} - \frac{1-\nu}{2} \frac{\partial^2 v_m}{\partial x^2} + \frac{m^2}{R^2} v_m - \frac{2h^2(1-\nu)}{12R^2} \frac{\partial^2 v_m}{\partial x^2} + \frac{h^2 m^2}{12R^4} v_m + \\ \frac{m}{R^2} w_m + \frac{h^2 m^3}{12R^4} w_m - \frac{h^2(2-\nu)m}{12R^2} \frac{\partial^2 w_m}{\partial x^2} + \frac{\rho_{str}(1-\nu^2)}{E} \frac{\partial^2 v_m}{\partial t^2} = 0 \end{aligned} \quad (1)$$

$$\begin{aligned} \frac{\nu}{R} \frac{\partial u_m}{\partial x} + \frac{m}{R^2} v_m + \frac{h^2 m^3}{12R^4} v_m - \frac{h^2(2-\nu)m}{12R^2} \frac{\partial^2 v_m}{\partial x^2} + \frac{1}{R^2} w_m + \frac{h^2}{12} \frac{\partial^4 w_m}{\partial x^4} \\ - \frac{2h^2 m^2}{12R^2} \frac{\partial^2 w_m}{\partial x^2} + \frac{h^2 m^4}{12R^4} w_m - \frac{\rho_{str}(1-\nu^2)}{E} \frac{\partial^2 w_m}{\partial t^2} + \frac{\rho_{fl}(1-\nu^2)R}{Eh} \frac{\partial \phi_m}{\partial t} = 0 \end{aligned}$$

The fluid's motion is governed by the velocity potential, $\phi_m(x, r, t)$, through the standard wave equation presented in (2) with cylindrical coordinates.

$$\frac{\partial^2 \phi_m}{\partial x^2} + \frac{\partial^2 \phi_m}{\partial r^2} + \frac{1}{r} \frac{\partial \phi_m}{\partial r} - \frac{m^2}{r^2} \phi_m - \frac{1}{c_{fl}^2} \frac{\partial^2 \phi_m}{\partial t^2} = 0 \quad (2)$$

and the continuity condition at the fluid-structure interface is given as

$$\frac{\partial \phi_m}{\partial r} = \frac{\partial w_m}{\partial t} \quad (3)$$

In these equations the m -spectrum has been uncoupled by utilising the axial symmetry of a cylindrical shell. The subscript, m , represents the circumferential wave-number. The axial, circumferential and radial displacements of the shell-surface are represented by u, v and w , respectively and are all axial x and time t dependent. The mechanical properties of the shell are governed by Young's modulus E , material density ρ_{str} and Poisson's ratio ν , whereas the fluid properties are governed by the fluid density ρ_{fl} and the fluid sound speed c_{fl} . Finally, the geometry of the shell is defined by the radius R and the thickness of the shell h .

To analyse the properties of free waves we derive the dispersion equation from (1-3) by means of the Fourier method and employ a space and time-harmonic ansatz, $\exp(kx - i\omega t)$, and in addition, a linear combination of Bessel-functions for the velocity potential. In the ansatz; ω is the angular frequency and k the axial wave-number. By substitution of the ansatz into the governing equations the linear differential equations reduce to linear algebraic equations from which the dispersion equation is found as the condition providing a non-trivial solution to the homogeneous linear equation system i.e. when the determinant is zero.

Confer to the chosen ansatz the equations are mapped into the frequency domain and the wave-numbers found at discrete frequencies as illustrated in Figure 1 for a steel-shell filled with water. The associated shell properties are given as: $R = 20$ mm, $h = 0.35$ mm, $E = 210$ GPa, $\nu = 0.3$, $\rho_{str} = 7800 \frac{\text{kg}}{\text{m}^3}$, $\rho_{fl} = 1000 \frac{\text{kg}}{\text{m}^3}$, $c_{fl} = 1440 \frac{\text{m}}{\text{s}}$ and vibrating in breathing mode, $m = 0$.

For further analysis, we introduce modal coefficients defined as the ratios of amplitudes of the axial and circumferential displacements to the amplitude of the radial displacement. These are referred to as α and β , respectively, and are found analytically by solving any two equations of

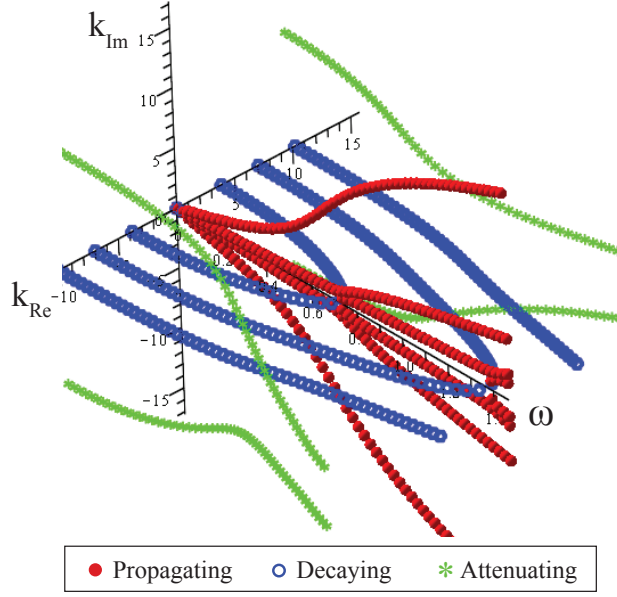


Figure 1. Dispersion of free waves for a fluid-filled shell vibrating in breathing mode, $m = 0$.

the linear system. The derivation of the dispersion equation and the modal coefficients can also be found in e.g. [3].

In addition to the continuity and motion equations the action integral includes a set of individually related generalised forces and displacements which are involved in the formulation of alternative boundary/loading conditions. The forces and displacements are related through the following complementary couples.

$$Q_{1m} \sim u_m \quad Q_{2m} \sim v_m \quad Q_{3m} \sim w_m \quad Q_{4m} \sim w'_m \quad p_m \sim \vartheta_m \quad (4)$$

where p_m is the acoustic pressure, ϑ the axial fluid velocity defined from the velocity potential as; $\vartheta = \frac{\partial \phi}{\partial x}$ and the generalised displacements, (u, v, w) , are defined by the ansatz with their generalised force counterparts also derived in [3] and defined as

$$\begin{aligned} Q_{1m} &= \frac{Eh}{1-\nu^2} \left[\frac{\partial u_m}{\partial x} + \frac{m\nu}{R} v_m + \frac{\nu}{R} w_m \right] \\ Q_{2m} &= \frac{Eh}{1-\nu^2} \left[-\frac{1-\nu}{2} \frac{m}{R} u_m + \frac{1-\nu}{2} \frac{\partial v_m}{\partial x} + \frac{h^2}{12} \frac{2(1-\nu)}{R^2} \frac{\partial v_m}{\partial x} + \frac{h^2}{12} \frac{2(1-\nu)m}{R^2} \frac{\partial w_m}{\partial x} \right] \\ Q_{3m} &= -\frac{Eh^3}{12(1-\nu^2)} \left[\frac{\partial^3 w_m}{\partial x^3} - \frac{(2-\nu)m^2}{R^2} \frac{\partial w_m}{\partial x} - \frac{(2-\nu)m}{R^2} \frac{\partial v_m}{\partial x} \right] \\ Q_{4m} &= \frac{Eh^3}{12(1-\nu^2)} \left[\frac{\partial^2 w_m}{\partial x^2} - \frac{m^2\nu}{R^2} w_m - \frac{m\nu}{R^2} v_m \right] \\ p_m &= \rho_{fl} \frac{\partial \phi_m}{\partial t} \end{aligned} \quad (5)$$

Furthermore, it can be shown that the free waves are orthogonal to each other and based on any two solutions to the governing equations in (1-3) we can apply the reciprocity theorem and derive the condition of orthogonality for a fluid-filled shell as shown in equation (6).

$$\begin{aligned} &Q_{1m}^{(n)} u_m^{(j)} + Q_{2m}^{(n)} v_m^{(j)} + Q_{3m}^{(n)} w_m^{(j)} + Q_{4m}^{(n)} w_m^{(j)'} + i \frac{R}{\omega} \int_0^1 p_m^{(n)} \vartheta_m^{(j)} \tilde{r} d\tilde{r} \\ &- Q_{1m}^{(j)} u_m^{(n)} - Q_{2m}^{(j)} v_m^{(n)} - Q_{3m}^{(j)} w_m^{(n)} - Q_{4m}^{(j)} w_m^{(n)'} - i \frac{R}{\omega} \int_0^1 p_m^{(j)} \vartheta_m^{(n)} \tilde{r} d\tilde{r} = 0 \end{aligned} \quad (6)$$

In the latter equation and hereafter we introduce the index-notation of (6) where the superscript refers to the axial wave-number and the subscript to the circumferential wave-number. Furthermore we introduce a scaling to the axial wave-number and the radial variable such that; $k_{\text{dim}} = \tilde{k}R^{-1}$ and $r_{\text{dim}} = \tilde{r}R$, however tilde is omitted in the following for brevity.

From the reciprocity relation used in the formulation of the orthogonality condition we can generalise to the power flow formulation by following the procedure in e.g. [1–3]. The individual power flow components given in (7) are expressed in terms of their generalised forces and displacements.

$$\begin{aligned}
N_m^{Axial} &= -\gamma_m \frac{\pi\omega R}{2} [\text{Re}(Q_{1m})\text{Im}(u_m) - \text{Im}(Q_{1m})\text{Re}(u_m)] \\
N_m^{Torsion} &= -\gamma_m \frac{\pi\omega R}{2} [\text{Re}(Q_{2m})\text{Im}(v_m) - \text{Im}(Q_{2m})\text{Re}(v_m)] \\
N_m^{Bending} &= -\gamma_m \frac{\pi\omega R}{2} [\text{Re}(Q_{3m})\text{Im}(w_m) - \text{Im}(Q_{3m})\text{Re}(w_m) \\
&\quad + \text{Re}(Q_{4m})\text{Im}(w'_m) - \text{Im}(Q_{4m})\text{Re}(w'_m)] \\
N_m^{Fluid} &= \gamma_m \frac{\pi R^2}{2} \int_0^1 [\text{Re}(p_m)\text{Im}(\vartheta_m) - \text{Im}(p_m)\text{Re}(\vartheta_m)] r dr \\
N_m^{Total} &= N_m^{Axial} + N_m^{Torsion} + N_m^{Bending} + N_m^{Fluid}
\end{aligned} \tag{7}$$

where $\gamma_{m=0} = 2$, $\gamma_{m \neq 0} = 1$ and N^{Axial} is the power flow carried in the axial components, $N^{Torsion}$ the power flow carried in the circumferential components etc.

3 MODAL DECOMPOSITION METHOD AND GREEN'S MATRIX

The governing equations presented in the previous section describes free vibrations for elastic fluid-filled cylindrical shells considered as multi-modal waveguides. This part of the analysis is a very well established subject and is carefully explored in e.g. [1, 2]. In contrast to the free vibrations it is usually of higher practical interest to treat forcing problems in fluid-filled shells. The general forcing problem is formulated from the governing equation (1) and (2) by introducing non-zero right-hand-sides, corresponding to mechanical and acoustical forcing, respectively. In this paper the forcing problems are solved by means of Green's matrix method and to ensure that any arbitrary forcing on the waveguide can be recovered, Green's matrix is formulated for five fundamental loading conditions (axial, circumferential, radial, flexural and acoustical) at each circumferential wave-number.

The conventional method of formulating Green's matrix is based on solving a system of complex simultaneous equations. Initially, the number of waves included in Green's matrix is truncated to M -waves and the number of symmetry conditions expanded accordingly to obtain M -equations associated with the M -waves. In [3] this is done by applying Galerkin's orthogonalisation procedure and orthogonalise e.g. the total pressure against individual velocity profiles. The complexity of this equation system does indeed affect the number of waves which can be retained in the analysis and in [4] only 7 are included to assess the response for acoustical excitations.

Unfortunately, 7 waves may not always provide a converged field and with a threshold in the range of 8 – 10 waves for this method, we are highly motivated for developing a new method providing an efficient formulation of Green's matrix. This can be achieved by means of the recent advances on bi-orthogonality conditions and a method based on modal decomposition which is outlined in the following.

3.1 Bi-orthogonality conditions

The bi-orthogonality conditions provide great potential for solving problems of time-harmonic forced vibrations in multi-modal waveguides. The bi-orthogonality conditions for a straight elastic layer has been derived in [5] and in [7] for an infinite elastic layer of uniform thickness. From this convenient reformulation of the conventional orthogonality condition the solution to the forced time-harmonic Rayleigh-Lamb problem is formulated by means of modal decomposition in [6] and the modal amplitudes can thus be found independently. The concept of bi-orthogonality is then further adapted to simple waveguides in [8] e.g. to an elastic cylindrical shell, also with the scope of calculating the modal amplitudes based on uncoupled algebraic equations rather than as a system of simultaneous equations.

The derivation of the bi-orthogonality conditions are based on discarding the case when $k_n = \pm k_j$ from the conventional orthogonality condition and arrive at two equations valid only for wave-numbers of different magnitude. Thus we are able to split the conventional orthogonality condition into two equally valid conditions, which, fortunately, always holds true for multi-modal waveguides. Further by subtraction of the two conditions we conveniently recover the original orthogonality condition of (6). Effectively the bi-orthogonality conditions can be interpreted as an advanced formulation of the reciprocity relation for multi-modal waveguides, which accounts for the fundamental symmetry properties of free waves. This is treated in detail in [7–9].

If we introduce an acoustic medium inside the shell treated in [8] the complexity of the equation system increase significantly and the derivation of the bi-orthogonality conditions become too comprehensive to be shown here. However, the necessary mathematical manipulations are similar to those conducted in [8] for the simple waveguides. Based on these manipulations the bi-orthogonality conditions for an elastic fluid-filled cylindrical shell are derived as in (8), to the authors knowledge, for the first time.

$$\begin{aligned}
 B1 : \quad & Q_{1m}^{(n)} u_m^{(j)} + Q_{4m}^{(n)} w_m^{(j)'} + i \frac{R}{\omega} \int_0^1 p_m^{(n)} \vartheta_m^{(j)} r dr = Q_{2m}^{(j)} v_m^{(n)} + Q_{3m}^{(j)} w_m^{(n)} \quad \text{for } k_n \neq \pm k_j \quad (8) \\
 B2 : \quad & (8) \quad n \leftrightarrow j
 \end{aligned}$$

where the second condition is recovered simply by interchanging the indices of the first condition.

3.2 Formulation of Green's matrix

In the formulation of Green's matrix the infinite shell is divided into two semi-infinite shells separated at the excitation point, ξ . The complete response of both semi-infinite domains are illustrated in (9) by introducing the module, $|x - \xi|$, in the ansatz.

$$\begin{aligned}
 u_m^{0N}(x, \xi) &= \sum_{j=1}^M u_m^{0N(j)} = \sum_{j=1}^M \alpha_m^{(j)} C_m^{0N(j)} \exp\left(\frac{k^{(j)}}{R} |x - \xi|\right) \\
 v_m^{0N}(x, \xi) &= \sum_{j=1}^M v_m^{0N(j)} = \sum_{j=1}^M \beta_m^{(j)} C_m^{0N(j)} \exp\left(\frac{k^{(j)}}{R} |x - \xi|\right) \\
 w_m^{0N}(x, \xi) &= \sum_{j=1}^M w_m^{0N(j)} = \sum_{j=1}^M C_m^{0N(j)} \exp\left(\frac{k^{(j)}}{R} |x - \xi|\right) \\
 \phi_m^{0N}(x, \xi, r) &= \sum_{j=1}^M \phi_m^{0N(j)} = \sum_{j=1}^M -i\omega R C_m^{0N(j)} J_m(\kappa^{(j)} r) \left[\frac{dJ_m(\kappa^{(j)} r)}{dr} \Big|_{r=1} \right]^{-1} \exp\left(\frac{k^{(j)}}{R} |x - \xi|\right)
 \end{aligned} \tag{9}$$

where κ is the radial wave-number, M the number of waves included, J_m the Bessel-function of first kind of order m and N indicates the five fundamental loading conditions, $N = 1, \dots, 5$.

3.2.1 Calculating modal amplitudes for mechanical excitations

Let us consider the third fundamental loading condition; a radial point source on the shell wall, applied at $x = \xi$ and distributed with the wave-number in the circumference as $\cos(m\theta)$. Obviously, the semi-infinite domains must satisfy continuity across the excitation point and a unit-jump in the real part of the excited component. This is ensured if the loading conditions in (10) are satisfied.

$$\begin{aligned} u_m^{03}(x, \xi) = 0 \quad \wedge \quad w_m'^{03}(x, \xi) = 0 \quad \wedge \quad v_m^{03}(x, \xi, r) = 0 \\ Q_{2m}^{03}(x, \xi) = 0 \quad \wedge \quad Q_{3m}^{03}(x, \xi) = -\frac{1}{2}\text{sgn}(x - \xi) \end{aligned} \quad \text{for } x \rightarrow \xi \quad (10)$$

Now, if we multiply each loading condition by their complementary generalised counterparts for a single mode, such that u_m^{03} is multiplied by the modal force $Q_{1m}^{03(n)}$, $w_m'^{03}$ by $Q_{4m}^{03(n)}$ etc. and sum the loading conditions according to the bi-orthogonality conditions we arrive at the algebraic equation of (11). Notice that the equations presented in the following are only valid at the point of excitation i.e. for $x \rightarrow \xi$, which is however omitted from the equations for brevity.

$$\begin{aligned} Q_{1m}^{03(n)} u_m^{03} + Q_{4m}^{03(n)} w_m'^{03} + i \frac{R}{\omega} \int_0^1 p_m^{03(n)} v_m^{03} r dr \\ - Q_{2m}^{03} v_m^{03(n)} - Q_{3m}^{03} w_m^{03(n)} = \frac{1}{2} \text{sgn}(x - \xi) w_m^{03(n)} \end{aligned} \quad (11)$$

where n indicates the n^{th} -modal generalised force/displacement and can be chosen arbitrarily.

By substitution of (9) into (11) we get

$$\begin{aligned} \sum_{j=1}^M \left[Q_{1m}^{03(n)} u_m^{03(j)} + Q_{4m}^{03(n)} w_m'^{03(j)} + i \frac{R}{\omega} \int_0^1 p_m^{03(n)} v_m^{03(j)} r dr \right. \\ \left. - Q_{2m}^{03(j)} v_m^{03(n)} - Q_{3m}^{03(j)} w_m^{03(n)} \right] = \frac{1}{2} \text{sgn}(x - \xi) w_m^{03(n)} \end{aligned} \quad (12)$$

This equation can now be simplified to (13) by applying the bi-orthogonality conditions from (8) as these explicitly states that for $k_n \neq \pm k_j$ the summation equates to zero. Thus we swap j with n and arrive at M -uncoupled equations, $n = 1, \dots, M$.

$$\begin{aligned} Q_{1m}^{03(n)} u_m^{03(n)} + Q_{4m}^{03(n)} w_m'^{03(n)} + i \frac{R}{\omega} \int_0^1 p_m^{03(n)} v_m^{03(n)} r dr \\ - Q_{2m}^{03(n)} v_m^{03(n)} - Q_{3m}^{03(n)} w_m^{03(n)} = \frac{1}{2} \text{sgn}(x - \xi) w_m^{03(n)} \end{aligned} \quad (13)$$

The interpretation of the latter equation is that each modal contribution is found individually and effectively the modes must form an independent set. Hence by employing the assumption of modal decomposition we arrive at the M algebraic equations of (13) and confer to the ansatz (using the Fourier method) the modal amplitudes can be expressed in the following simple form.

$$C_m^{03(n)}(\omega) = \frac{1}{2} \text{sgn}(x - \xi) [F_m^{(n)}(\omega)]^{-1} \quad (14)$$

where $F_m^{(n)}(\omega)$ is given as the left-hand-side of (13) with the amplitudes sorted out of each individual term as seen in (15).

$$\begin{aligned}
F_m^{(n)}(\omega) = & \\
(Q_{1m}u_m) : & \frac{Eh}{1-\nu^2} \left[\frac{\text{sgn}(x-\xi)}{R} k^{(n)} \alpha_m^{(n)} + \frac{m\nu}{R} \beta_m^{(n)} + \frac{\nu}{R} \right] \alpha_m^{(n)} \\
(Q_{2m}v_m) : & -\frac{Eh}{1-\nu^2} \left[\frac{1-\nu}{2} \frac{1}{R} (\text{sgn}(x-\xi) k^{(n)} \beta_m^{(n)} - m \alpha_m^{(n)}) \right. \\
& \left. + \text{sgn}(x-\xi) \frac{h^2}{12} \frac{2(1-\nu)}{R^3} k^{(n)} (\beta_m^{(n)} + m) \right] \beta_m^{(n)} \\
(Q_{3m}w_m) : & + \text{sgn}(x-\xi) \frac{Eh^3}{12(1-\nu^2)} \left[\frac{1}{R^3} (k^{(n)})^3 - \frac{(2-\nu)m^2}{R^3} k^{(n)} - \frac{(2-\nu)m}{R^3} k^{(n)} \beta_m^{(n)} \right] \\
(Q_{4m}w'_m) : & + \frac{Eh^3}{12(1-\nu^2)} \left[\frac{1}{R^2} (k^{(n)})^2 - \frac{m^2\nu}{R^2} - \frac{m\nu}{R^2} \beta_m^{(n)} \right] \frac{\text{sgn}(x-\xi)}{R} k^{(n)} \\
(p_m\vartheta_m) : & -\text{sgn}(x-\xi) \rho_{fl} \omega^2 R^2 k^{(n)} \left[\frac{dJ_m(\kappa^{(n)}r)}{dr} \Big|_{r=1} \right]^{-2} \int_0^1 J_m(\kappa^{(n)}r)^2 r dr
\end{aligned} \tag{15}$$

As a final remark, notice that $k^{(n)}$ and $\kappa^{(n)}$ are implicit functions of ω and m and further that the integral in (15) is Lommel's integral, which reduce to a simple algebraic expression as well. Thus we have derived a simple, purely algebraic, equation, from which all modal amplitudes can be determined by substitution of the angular frequency, the circumferential wave-number and the associated axial wave-number.

For the remaining mechanical loading conditions the procedure is completely analogue and the governing equations for calculating the modal amplitudes become

$$\begin{aligned}
Q_{1m}^{01(n)} u_m^{01(n)} + Q_{4m}^{01(n)} w_m'^{01(n)} + i \frac{R}{\omega} \int_0^1 p_m^{01(n)} \vartheta_m^{01(n)} r dr \\
- Q_{2m}^{01(n)} v_m^{01(n)} - Q_{3m}^{01(n)} w_m^{01(n)} = -\frac{1}{2} \text{sgn}(x-\xi) u_m^{01(n)} \\
(16) = \frac{1}{2} \text{sgn}(x-\xi) v_m^{02(n)} \\
(16) = -\frac{1}{2} \text{sgn}(x-\xi) w_m'^{04(n)}
\end{aligned} \tag{16}$$

By comparing these with (13) it is seen that only the right-hand-side change and consequently this allow us to determine the remaining mechanical modal amplitudes based on the modal amplitudes from the radial loading condition alone.

$$\begin{aligned}
C_m^{01(n)}(\omega) &= -\alpha_m^{(n)} C_m^{03(n)}(\omega) \\
C_m^{02(n)}(\omega) &= \beta_m^{(n)} C_m^{03(n)}(\omega) \\
C_m^{04(n)}(\omega) &= -\frac{\text{sgn}(x-\xi)}{R} k^{(n)} C_m^{03(n)}(\omega)
\end{aligned} \tag{17}$$

Thus the modal amplitudes for all mechanical excitations are determined based on the single algebraic equation of (14) and in addition simple multiplication operations.

3.2.2 Calculating modal amplitudes for acoustical excitations

For the acoustical excitations the source is introduced as a ring source profiled as the mechanical sources in the circumference, concentrated at $x = \xi$ and applied at the radius r_0 . To evaluate the

difference in the near field energy distribution between applying a pressure and a velocity ring source both sources are applied as excitations in this paper. The acoustical ring source excitations are represented by the delta-function, $\delta(r - r_0)$, and due to the radial and axial dependence of the velocity potential the loading is introduced as in (18) in contrast to the mechanical excitation (radial independent) shown in (10).

$$\begin{aligned} p_m^{05}(x, \xi, r) &= i\omega\rho_{fl}\frac{1}{2r_0}\delta(r - r_0)\text{sgn}(x - \xi) \\ \vartheta_m^{06}(x, \xi, r) &= -\frac{1}{2r_0}\delta(r - r_0)\text{sgn}(x - \xi) \end{aligned} \quad \text{for } x \rightarrow \xi \quad (18)$$

where the velocity excitation can be interpreted as a monopole source and as the pressure is a normal directed force the pressure excitation can be interpreted as a dipole source when the sign-function is included.

By the same analogy the governing equations for calculating the modal amplitudes for acoustical excitations are given in (19).

$$\begin{aligned} Q_{1m}^{05(n)}u_m^{05(n)} + Q_{4m}^{05(n)}w_m'^{05(n)} + i\frac{R}{\omega}\int_0^1 p_m^{05(n)}\vartheta_m^{05(n)}rdr \\ -Q_{2m}^{05(n)}v_m^{05(n)} - Q_{3m}^{05(n)}w_m^{05(n)} = -\text{sgn}(x - \xi)\frac{\rho_{fl}R}{2r_0}\int_0^1 \delta(r - r_0)\vartheta_m^{05(n)}rdr \\ = -\text{sgn}(x - \xi)\frac{\rho_{fl}R}{2}\vartheta_m^{05(n)}\Big|_{r=r_0} \end{aligned} \quad (19)$$

$$(19) \stackrel{05 \Rightarrow 06}{=} -i\text{sgn}(x - \xi)\frac{R}{2\omega}p_m^{06(n)}\Big|_{r=r_0} \quad (20)$$

and by substitution of the generalised pressure and velocity the modal amplitudes are determined as

$$\begin{aligned} C_m^{05(n)}(\omega) &= ik^{(n)}R\omega\rho_{fl}J_m(\kappa^{(n)}r)\Big|_{r=r_0}\left[\frac{dJ_m(\kappa^{(n)}r)}{dr}\Big|_{r=1}\right]^{-1}C_m^{03(n)}(\omega) \\ C_m^{06(n)}(\omega) &= i\text{sgn}(x - \xi)R^2\omega\rho_{fl}J_m(\kappa^{(n)}r)\Big|_{r=r_0}\left[\frac{dJ_m(\kappa^{(n)}r)}{dr}\Big|_{r=1}\right]^{-1}C_m^{03(n)}(\omega) \end{aligned} \quad (21)$$

By inspection of the modal amplitudes for the acoustical excitations it is evident that the relation between these and the modal amplitudes for the mechanical excitations are once again just a simple multiplier.

In conclusion, the modal decomposition method allow us to express the modal amplitudes for all fundamental loading conditions explicitly and through a convenient analytic algebraic equation, dependent on the angular frequency, the circumferential wave-number and the associated axial wave-number. Based on this formulation we are able to include an arbitrarily large number of waves in Green's matrix provided that all wave-numbers associated with m and ω are available.

Furthermore, this method is very strong as the modal amplitudes are found independent of the number of waves we wish to include in the analysis, however as a compromise the symmetry conditions are satisfied only as $M \rightarrow \infty$ and the convergence of this method is thereby related to convergence of the symmetry conditions rather than convergence of the modal amplitudes.

4 VERIFICATION AND CONVERGENCE

To validate the modal decomposition method the obvious choice would be a qualitative experimental set-up, however due to time constraints this has not been conducted for fluid-filled pipes at this point. Nonetheless, as the conventional method is well established and accepted, the modal decomposition is validated against the results obtained in [3] for mechanical excitations. For the acoustical excitations no paper contains, to the authors knowledge, a converged near field energy distribution for acoustical excitations and therefore these are validated through a convergence study.

4.1 Verification of the modal decomposition method

To ensure that the modal decomposition method is valid for mechanical excitations, it is compared to the power flow graphs presented in [3] using the same physical parameters (presented in section 2 of this paper) and with 20 waves included. Through a comparison between the graphs illustrated in [3] pp. 843-844, Fig. 15 and 16, for three mechanical excitations and the graphs illustrated in Figure 2, it is evident that the near field distributions are all identical. This effectively means that we can obtain converged energy distributions for mechanical excitations in fluid-filled shells with a low number of waves retained.

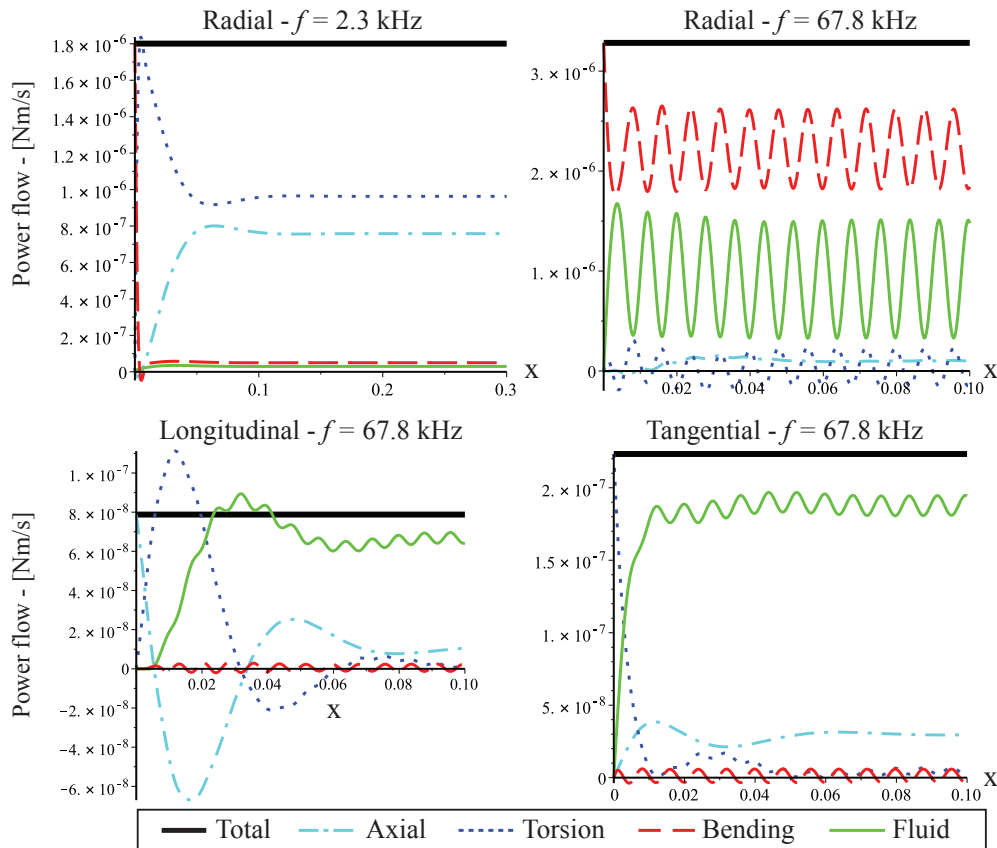


Figure 2: Near field energy distribution with 20 waves included, $m = 3$, and evaluated at $f = 2.3$ kHz and $f = 67.8$ kHz - just after the first and second cut-on frequency. The verification graphs can be found in [3] on pp. 843-844, Fig. 15 and 16.

In [4] the energy distribution is considered for acoustical excitations as well, however with only 7 waves included. Through the convergence study in section 4.2 it is clear that 7 waves does not provide a converged energy distribution and confer to the differences between the conventional method and the modal decomposition method, it can not be justified to compare the energy fields of the two, even though the same number of waves are included.

This is simply due to the fact that the essential conditions from the view point of the conventional method is symmetry, whereas the essential part from the view point of the modal decomposition method is each modal contribution independent of each other. Thus in the conventional method the symmetry conditions are ensured by choosing the amplitudes 'artificially' through a weighted averaged where the weighting is determined by the physical parameters of the shell. Consequently, for the non-converged case illustrated in [4] the amplitudes are scaled unintentionally corresponding to the weighting, hence the amplitudes will deviate from those calculated by means of the modal decomposition method and a comparison would be pointless.

4.2 Convergence study

To ensure that the modal decomposition method is valid for acoustical excitations as well the convergence of the symmetry conditions are studied in the following, however, only presented here for the acoustical velocity excitation at the excitation frequency, $f = 66.7$ kHz.

Initially, it is of interest to validate that the load converges towards the delta-function at the point of excitation. In Figure 3 the distribution of the fluid velocity, $\vartheta_m(x, \xi, r)$, is shown across the radii for an increasing number of waves at $m = 3$ and evaluated at the point of excitation, $x = \xi$, with the delta-function applied at $r_0 = 0.5$.

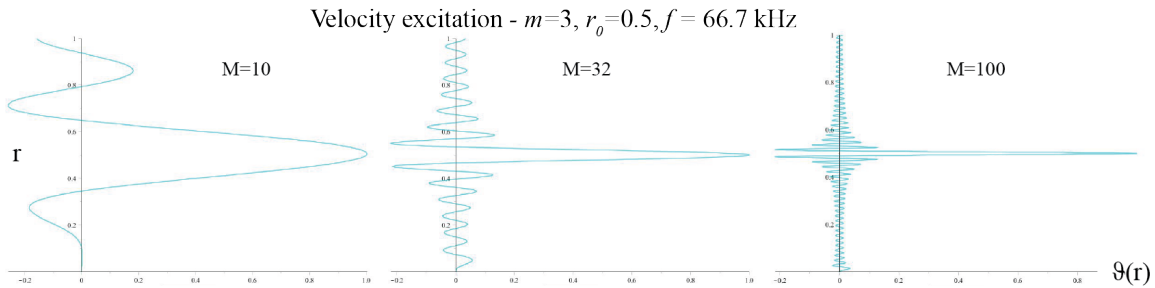


Figure 3: Convergence of the applied excitation, $\vartheta(r)$, across the radii for an increasing number of waves. Normalised with respect to the intensity at the excitation point, $r_0 = 0.5$.

Based on this figure it is easily verified that for an increasing number of waves the source distribution resembles the delta-function. Similarly, this also holds true for all other circumferential wave-numbers and locations of the source.

With convergence of the load verified it is of interest to study the convergence of the symmetry conditions. Through the derivation of the modal decomposition method each modal contribution is derived explicit and independent on the number of retained waves, hence the study of convergence is related to the symmetry conditions and not the amplitudes. This immediately provides us with four distinct and readily available convergence parameters, for which we can determine a threshold based on desired numerical accuracy. To verify that the modal decomposition method is applicable for acoustical loadings as well, the four symmetry conditions for the acoustical velocity excitation located slightly from the fluid-structure interface, at $r_0 = 0.95$, are shown in Figure 4 for an increasing number of waves.

From the figure it is seen that Q_2 and u converges must faster than Q_3 and w' , which can easily be visualised by plotting the generalised forces and displacements as a continuous function of the wave-number. The same can be conducted in case of a pressure excitation by visualising their symmetry conditions, w and Q_4 , continuously along the wave-number. From the physical view point the slow convergence of these flexural components are governed by the distinct differences in the membrane and flexural stiffness and effectively the flexural components are more sensitive to the acoustical sources. In conclusion the convergence parameters reduce conveniently from four to two parameters.

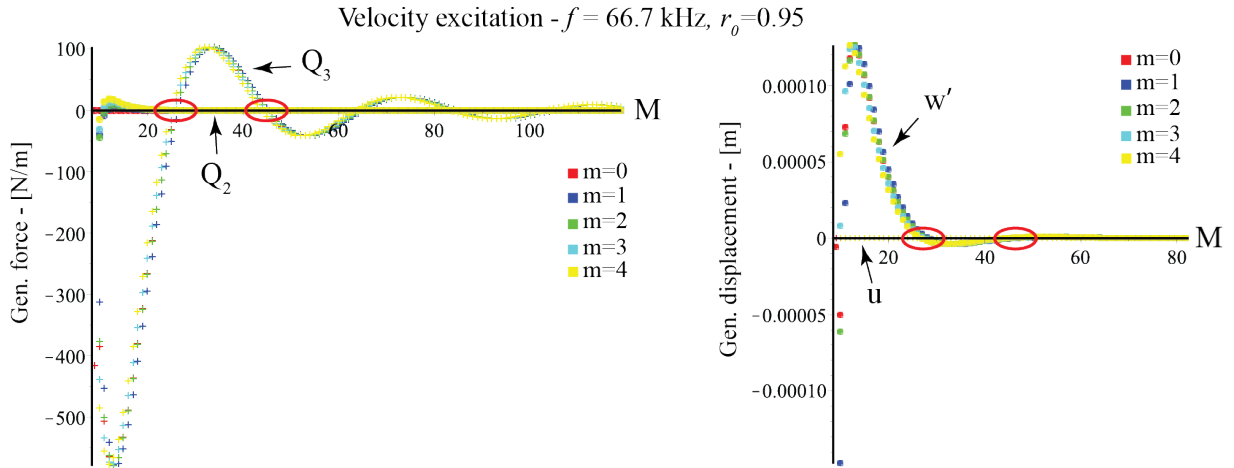


Figure 4: Convergence of the symmetry conditions for an acoustical velocity excitation located at $r_0 = 0.95$.

Furthermore, it is clear that the symmetry conditions converge non-monotonic towards zero and through similar studies it is found that the oscillating behaviour holds true independent of the source location and circumferential wave-number. Fortunately, the forces and displacements will oscillate in a similar manner causing common intersections points as indicated in Figure 4. Thus it may be advantageous to choose the number of waves for future analysis based on a convergence study of the generalised forces and displacements as this will provide the best compromise between a low number of waves but converged symmetry conditions. On the other hand, this will not necessarily provide a converged velocity potential. Nevertheless, for the case shown in Figure 4 with the physical parameters of section 2, the excitation located at $r_0 = 0.95$ and excited at 66.7 kHz, a qualitative number of waves for the proceeding analysis will be $M = 25$.

For mechanical excitations the convergence study is also conducted by means of the symmetry conditions and further, for mechanical excitations, it applies that the introduced load must be recovered by summation of all modal forces in the loaded direction. Thus for mechanical excitations there are five distinct convergence parameters and dependent on the physical parameters these are converged with 7 – 10 waves retained.

In conclusion, the difference in the number of waves necessary to obtain a converged energy field for mechanical and acoustical excitations are anticipated to be a consequence of the load introduction. For mechanical excitations we introduce a finite-valued source but for the acoustical excitations the load is introduced as a delta-function and in effect it will excite a wider spectrum of waves with a significant amplitude - including higher order modes as well.

5 RESULTS AND DISCUSSION

To illustrate advantages of the proposed methodology we present here results of some case-studies.

5.1 Analysis of acoustical excitations of an elastic fluid-filled cylindrical shell

In extension to the previous section we investigate performance of the shell considered in [3] in case of acoustical excitations i.e. with pressure and velocity sources. In Figure 5 the near field energy distribution is shown for the velocity and pressure excitations applied at $r_0 = 0.95$ - both normalised with their respective total energy.

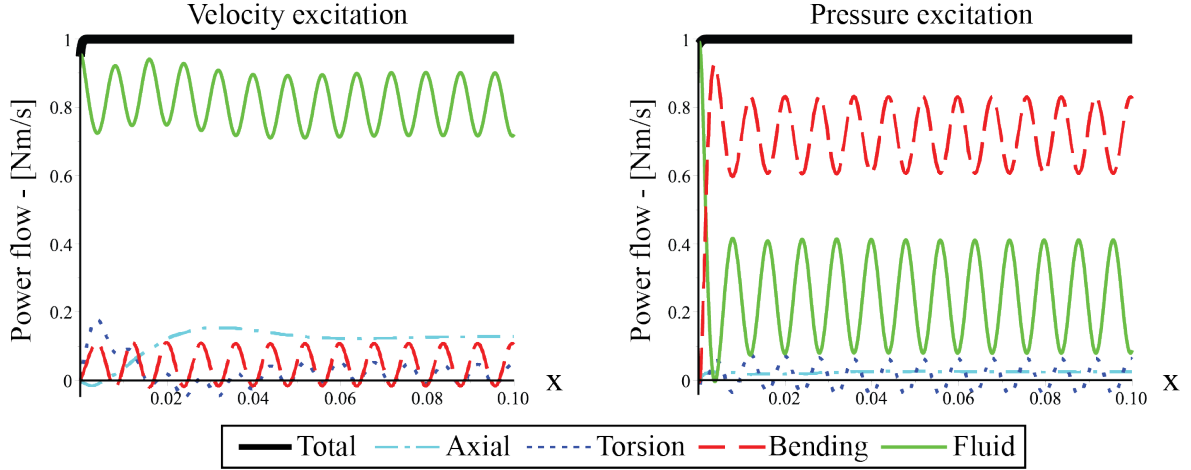


Figure 5: Near field energy distribution for velocity and pressure excitations at $r_0 = 0.95$ with an excitation frequency of 67.8 kHz at $m = 3$ and 25 waves retained. Normalised individually with the total energy.

This energy distribution reveals that with a velocity excitation 70-90% of the energy is trapped in the fluid, whereas with the pressure excitation the fluid energy escapes rapidly to the shell in terms of bending energy, which then carries 60-90% of the energy. In effect a pressure excitation close to the interface is comparable to a mechanical loading and has a distribution similar to that of a flexural excitation, however with another near field characteristic.

On the other hand, as the source is located further from the interface the energy distribution with a pressure excitation turns towards the distribution with a velocity excitation as illustrated in Figure 6. At this location approximately 80% of the energy remains in the fluid for both excitations, when the sources are located $\frac{1}{4}$ from the fluid-structure interface. However, in the pressure excitation with a slightly more pronounced oscillating fluid energy component but as the source moves closer to the centre the oscillating behaviour of the fluid energy vanishes and the energy distribution from the two sources become similar.

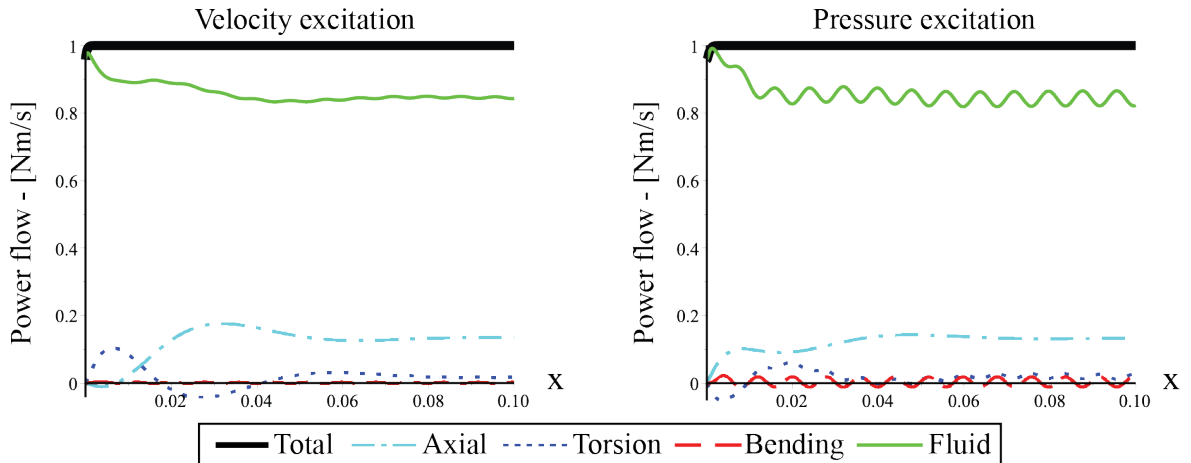


Figure 6: Near field energy distribution with velocity and pressure excitations $\frac{1}{4}$ from the fluid-structure interface, an excitation frequency of 67.8 kHz at $m = 3$ and 25 waves retained. Normalised individually with the total energy.

As a concluding remark, it is also possible to evaluate the energy distribution when the source is located in the centre, $r_0 = 0$, as the velocity potential is defined to ensure a bounded solution at $r \rightarrow 0$. At this point the source transforms from a ring source to a point sources and if the energy distribution for such an acoustical excitation is evaluated it is seen that the energy is carried

solely in breathing mode and further, that it is comparable to a longitudinal mechanical excitation vibrating in breathing mode. The overall difference is simply that the energy travels inside the fluid rather than in the axial component of the shell.

5.2 Other useful properties of the bi-orthogonality conditions

As demonstrated, the bi-orthogonality conditions are highly relevant in calculating the modal amplitudes for a set of fundamental loading conditions and effectively in the formulation of Green's matrix as well. On the other hand, through the development of this method it has been discovered that the bi-orthogonality conditions also contains potential in finding the wave-numbers, which conventionally are found from the dispersion equation.

What has been detected through the work documented in this paper is actually that certain fluid-originated roots are "hidden" in the dispersion equation, meaning that the convergence rate of these wave-numbers is very poor. Thus the bi-orthogonality conditions can be facilitated as an alternative formulation for finding these roots.

The "only" requirement for one of the bi-orthogonality conditions to act as a replacement for the dispersion equation is that an arbitrary wave-number, k_j , which satisfies the governing equations of (1-3) is available. The idea is simply to calculate any other wave-number, k_n , by require that it satisfies the bi-orthogonality conditions with respect to the already known wave-number, k_j , i.e. the wave-numbers must be bi-orthogonal so to say. Substituting the frequency and known wave-number into equation (8) will provide us with a continuous function in k_n which seems to be more smooth than the original dispersion equation and may therefore be convenient from the view point of convergence rate.

What is however interesting is that the characteristic of this equation change according to whether the known wave-number is substituted into k_j or k_n and similar, through a concise investigation, it seems that specific sets of wave-numbers become more pronounced in the equation depending on whether the known wave-number is purely imaginary, purely real or complex. This immediately entails for a further investigation to clarify whether wave-numbers are more pronounced in the bi-orthogonality conditions.

6 RESPONSE OF A FLUID-FILLED SHELL TO THE EXCITATION DEFINED BY DATA FROM CFD-MODELLING OF AN OPERATING PUMP

The practical purpose of this paper is to reliably predict the vibro-acoustic performance of a pump. To accomplish this, the output from an extensive CFD analysis of an operating pump should be 'mapped' onto the vibro-acoustic model developed in this paper. Thereby the near field energy distribution can be assessed when the waveguide is subjected to certain CFD velocity or pressure profiles. This conveniently allows for a source characterisation and thorough analysis of the transmission path(s) for such pressure and/or velocity pulsations.

Initially, the time-dependent CFD-data needs to be transformed from the time-domain into the frequency domain, where our vibro-acoustic model is defined. This transformation is to be conducted for each nodal value of the CFD-data and is done by means of a (fast) Fourier transformation. The succeeding step is to adjust this frequency dependent data to the modal decomposition of the model. The CFD-data is then decomposed in the circumferential direction at individual circumferential wave-numbers through a Fourier series. Thus we decompose the CFD-data into separate branches of data for each retained circumferential wave-number. Hence if the branches are summarised over the retained circumferential wave-numbers we recover the original CFD-data in the frequency domain.

Then by similar data processing for the radial distribution at each circumferential wave-number we are able to predict the acoustical sources in the CFD-data and evaluate the vibro-acoustic per-

formance of an operating pump by means of Green's matrix method. This is the subject of our on-going work.

7 CONCLUDING REMARKS

Through this paper a highly efficient tool, the bi-orthogonality conditions, has been facilitated to decompose the governing equation system which allows us to express the modal amplitudes explicitly and independently of each other via the excitation frequency, circumferential wave-number and the associated axial wave-number. Further, simple relations between the modal amplitudes from different fundamental loading conditions has been detected, which effectively reduce the equations for calculating the modal amplitudes of all fundamental loading conditions to only one simple algebraic equation and simple multiplication operations.

This very strong method directly allows for assessing the near field energy distribution and obtain converged solutions for both mechanical and acoustical excitations. To validate that the modal decomposition method applies, the case of mechanical excitations are verified against identical loadings in [3] and for the acoustical excitations no qualitative reference models have been found, hence these loadings are validated through a convergence study of the applied delta-function and the symmetry conditions.

Through the development of this method it has also been discovered that the bi-orthogonality conditions may be utilised as a 'root-finder' in favour of the conventional dispersion equation. At this point, this is however not investigated in substantial detail and is thereby left for future works.

REFERENCES

- [1] G. Pavić. Vibrational energy flow in elastic circular cylindrical shells. *J. Sound and Vibration*, 142:293–310, 1990.
- [2] C. R. Fuller and F. J. Fahy. Characteristics of wave propagation and energy distributions in cylindrical elastic shells filled with fluid. *J. Sound and Vibration*, 81:501–518, 1982.
- [3] S. V. Sorokin, J. B. Nielsen, and N. Olhoff. Green's matrix and the boundary integral equation method for the analysis of vibration and energy flow in cylindrical shells with and without internal fluid. *J. Sound and Vibration*, 271:815–847, 2004.
- [4] S. V. Sorokin and A. V. Terentiev. Flow-induced vibrations of an elastic cylindrical shell conveying a compressible fluid. *J. Sound and Vibration*, 296:777–796, 2006.
- [5] Y. I. Bobrovnikskii. Orthogonality relations for lamb waves. *Soviet Acoustical Physics*, 18:432–433, 1973.
- [6] Baruch Karp. Generation of symmetric lamb waves by non-uniform excitations. *J. Sound and Vibration*, 312:195–209, 2008.
- [7] J. D. Achenbach. *Reciprocity in elastodynamics*. Second. Cambridge University Press, 2003.
- [8] Sergey V. Sorokin. On the bi-orthogonality conditions for multi-modal elastic waveguides. *J. Sound and Vibration*, 332:5606–5617, 2013.
- [9] D. D. Zakharov. Orthogonality of 3d guided waves in viscoelastic laminates and far field evaluation to a local acoustic source. *J. Solids and Structures*, 45:1788–1803, 2008.